JGR Oceans

Characterization of the CO_2 System in a Coral Reef, a Seagrass Meadow, and a Mangrove Forest in the Central Red Sea

Vincent Saderne[1] (iD), Kimberlee Baldry[1,2] (iD), Andrea Anton[1] (iD), Susana Agustí[1] (iD), and Carlos M. Duarte[1] (iD)

[1]Red Sea Research Centre and Computational Bioscience Research Center, King Abdullah University of Science and Technology, Thuwal, Saudi Arabia, [2]Institute for Marine and Antarctic Studies, University of Tasmania, Hobart, Australia

Abstract The Red Sea is characterized by its high seawater temperature and salinity, and the resilience of its coastal ecosystems to global warming is of growing interest. This high salinity and temperature might also render the Red Sea a favorable ecosystem for calcification and therefore resistant to ocean acidification. However, there is a lack of survey data on the CO_2 system of Red Sea coastal ecosystems. A 1-year survey of the CO_2 system was performed in a seagrass lagoon, a mangrove forest, and a coral reef in the central Red Sea, including fortnight seawater sampling and high-frequency pH_T monitoring. In the coral reef, the CO_2 system mean and variability over the measurement period are within the range of other world's reefs with pH_T, dissolved inorganic carbon (DIC), total alkalinity (TA), pCO_2, and Ω_{arag} of 8.016 ± 0.077, 2061 ± 58 $\mu mol/kg$, 2415 ± 34 $\mu mol/kg$, 461 ± 39 μatm, and 3.9 ± 0.4, respectively. Here, comparisons with an offshore site highlight dominance of calcification and photosynthesis in summer-autumn, and dissolution and heterotrophy in winter-spring. In the seagrass meadow, the pH_T, DIC, TA, pCO_2, and Ω_{arag} were 8.00 ± 0.09, 1986 ± 68 $\mu mol/kg$, 2352 ± 49 $\mu mol/kg$, 411 ± 66 μatm, and 4.0 ± 0.3, respectively. The seagrass meadow TA and DIC were consistently lower than offshore water. The mangrove forest showed the highest amplitudes of variation, with pH_T, DIC, TA, pCO_2, and Ω_{arag}, were 7.95 ± 0.26, 2069 ± 132 $\mu mol/kg$, 2438 ± 91 $\mu mol/kg$, 493 ± 178 μatm, and 4.1 ± 0.6, respectively. We highlight the need for more research on sources and sinks of DIC and TA in coastal ecosystems.

Plain Language Summary Global warming and ocean acidification are consequences of increased CO_2 emissions to the atmosphere by humankind and are major threats to marine ecosystems. The Red Sea waters are naturally warm and saline. The resilience of its coral reefs, mangrove forests, and seagrass meadows is of growing interest for the scientific community in the context of global warming. The high temperature and salinity might render the Red Sea quite resistant to ocean acidification as well as an environment chemically very favorable for calcification, notably by corals. Calcification is a process dampened by the acidity (pH) of water, which depends on the chemistry of CO_2 in seawater. Warm and saline water naturally tend to have a more basic pH and then be less corrosive to calcareous skeletons. However, the chemistry of the CO_2 and acidity baselines and variability in the Red Sea are poorly documented. We conducted a year-round survey of the CO_2 chemistry of seawater in a seagrass meadow, mangrove forest, and coral reef ecosystem, involving discrete water sampling and high-frequency measurements.

1. Introduction

Increasing anthropogenic carbon dioxide (CO_2) emissions have led to a global increase in atmospheric CO_2 concentration over the past two decades, causing global warming and a decrease of seawater pH known as ocean acidification (OA; e.g., Orr, 2011). Separately or in combination, warming and OA are considered major threats to marine systems (e.g., Harvey et al., 2013), particularly to coral reefs, suffering recurrent wide-scale bleaching in recent years due to major heatwave events (Hughes et al., 2017).

Hence, understanding the resilience of organisms and ecosystems naturally exposed to permanent or periodical extreme conditions of temperature and partial pressure of CO_2 (pCO_2) is of particular interest (Camp et al., 2018). The Red Sea is one of the hottest seas on the planet, with mean annual maximum sea surface temperatures above 30 °C in the central and southern parts (Chaidez et al., 2017), providing an extreme

temperature environment for coral reefs. Nevertheless, Red Sea corals are vulnerable to thermal stress, with the 2015 global coral bleaching event leading to mass mortality south of 20°N (Hughes et al., 2018; Monroe et al., 2018).

Besides homing extensive coral reefs, the Red Sea is also a global hotspot of seagrass diversity (Kenworthy et al., 2006). Moreover, the sea surface temperature above 20 °C in winter allows the presence of mangrove forests along most of its coastline (Almahasheer et al., 2016). However, mangroves face adverse conditions for growth, due to lack of freshwater run-off, salinity over 40, and nutrient limitation (Almahasheer et al., 2016).

The Red Sea is unlikely to be vulnerable to OA due to its high water temperature, salinity and total alkalinity (TA) favoring high saturation states for carbonate minerals (e.g., Takahashi et al., 2014). On the other hand, the high temperature of the seawater leads to low pH (all other parameters constants) due to the increased activity of hydrogen ions (Hunter, 1998). Thus, the coastal ecosystems of the Red Sea, particularly coral reefs, might be exposed to a unique CO_2 system in terms of both the baseline and variability. The CO_2 system of Red Sea coastal ecosystems has been so far poorly studied. The only available data on the carbonate system of Red Sea in coral reefs derive from the Gulf of Aqaba, the coldest area of the Sea (Silverman et al., 2007).

Recently, Hughes et al. (2017) advocated for the need to test for "realistic" OA future scenarios using $p\mathrm{CO_2}$ around 450 µatm, corresponding to pH in the range of 7.9–8.1. However, these projections apply to the open ocean and do not consider coastal ocean conditions, where vulnerable organisms reside, and subject to strong fluctuations in $p\mathrm{CO_2}$. These highly dynamic CO_2 systems are observed due to the ecosystems metabolism and inputs of freshwater and alkalinity from the watershed (Duarte et al., 2013; Wahl et al., 2015). As such, there is a need to characterize the CO_2 system and natural variability of coastal ecosystems to inform realistic ecosystem-specific high $p\mathrm{CO_2}$ experiments (e.g., Andersson & MacKenzie, 2012; Fassbender et al., 2016; Rivest et al., 2017). Different coastal ecosystems (coral reefs, seagrass and seaweed meadows, and mangrove forests) have complex CO_2 system baseline and variability, due to their different community and sediment structure (Challener et al., 2016; Cyronak et al., 2018; Cyronak et al., 2018; Rosentreter et al., 2018).

The present study aims to characterize the baseline CO_2 system in three key benthic ecosystems of the central Red Sea over one year; a mangrove forest, a seagrass meadow, a coral reef and an additional offshore site as a reference for comparison. We aimed at characterizing (1) the seasonal and diel variations of the CO_2 system and (2) the potential drivers of TA and dissolved inorganic carbon (DIC) at each ecosystem. The pH was surveyed at high resolution using SeaFET sensors and water samples were taken every second week for the full characterization of the CO_2 system.

2. Material and Methods

2.1. Sites, Sampling, and Measurements

The three study sites were located at a coral reef, a mangrove forest and a seagrass meadow in the central Red Sea (Figure 1). The sensor packages for the benthic moorings were composed of a SeaFET pH sensor (Sea Bird Scientific, Halifax, Canada; Martz et al., 2010) and a salinity - temperature - depth multiparametric sensor (CTD) equipped with a central wiping device (EXO2, YSI Inc., Yellow Springs, USA). The pH on the total scale (pH_T) was recorded at a frequency of 5 to 10 min and CTD with a frequency of 10 min. The coral reef site was located on the inner slope of the backreef of Al-Fahal reef (22°14′59″N, 38°57′45″E), a 14 km long barrier-type reef about 12 km offshore and marking the transition with open sea. The sensors were attached to a frame vertically on a reef spur, their sensing head approximately 120 cm above the sandy bottom. The seagrass meadow site was located in an extensive *Enhalus acoroides* meadow in the Khor Almesena′a coastal lagoon (22°23′50″N, 39°08′06″E). The sensors were moored within the meadows canopy on a metallic pole anchored to the sediment, their sensing head approximately 55 cm above the sediment. The mangrove forest site was located at the fringe of a dwarf mangrove stand (*Avicennia marina*; 22°20′21″N, 39°05′19″E). Transparent sections of polycarbonate pipes were buried vertically to create casings in the sediment. The CTD and SeaFET sensors were positioned vertically in the pipes sensing heads up. To protect the SeaFET sensing head from
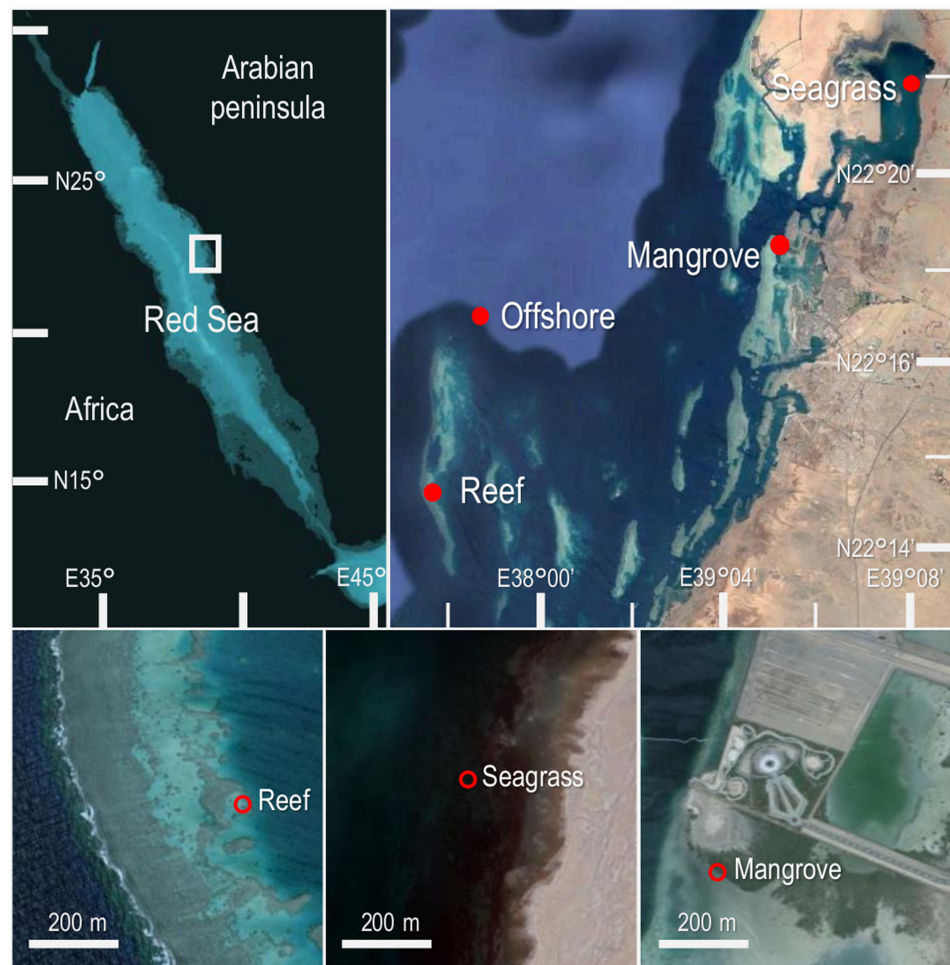
Figure 1. Deployment maps.

desiccation at low tide, a transparent cylindrical cut was glued to the top of the SeaFET head (as a sleeve), protruding approximately 15 cm from sediment. We considered that the SeaFET was not capable of measuring pH when the CTD was not able to measure salinity (water level < 20 cm).

The time series sampling took place from summer 2016 to summer 2017. The SeaFET moorings were from 6 September 2016 to 23 August 2017 in the seagrass meadow site and, in the mangrove forest site, from 16 August 2016 to 19 August 2017 with an interruption between 23 and 31 October 2016. At the coral reef site, the SeaFET mooring started 16 June 2016 and was interrupted 9 May 2017 because of sensor malfunction, with three interruptions for maintenance, between 31 August 2016 and 30 September 2016, 11 and 18 November 2016 and 27 and 30 March 2017. The CTD moorings were conducted in parallel to the SeaFET moorings. At the seagrass meadow site, a malfunction of the CTD caused a gap of data between 12 November 2016 and 20 January 2017, two more interruptions for maintenance occurred between 3 and 9 March 2017 and between 11 and 20 June 2017. At the coral reef site, two interruptions for maintenance occurred between 5 and 17 November 2017 and between 3 and 9 June 2017.

Discrete seawater samples for TA, DIC, and pH_T measurements, as well as samples for total phosphate and silicate, were taken approximately every second week at the head of the SeaFET in the coral reef (29 June 2016 to 23 August 2017) and seagrass meadow (20 September 2016 to 23 August 2017) sites and at the peak of high tide at noon at the mangrove forest site (7 September 2016 to 14 August 2017). Sampling and storage of the samples for determination of the CO_2 system was performed according to the standard operating procedures described in Dickson et al. (2007). Additionally, water samples were taken every 15 days at a offshore reference site (22°18′33″N, 38°59′50″E) at 1-m depth using a Niskin bottle. The salinity and temperature

were recorded at the time of sampling using a calibrated Ocean Seven 305 Plus multiparameter sonde (Idronaut S.r.I, Brugherio, Italy). The offshore reference site did not have a SeaFET sensor.

2.2. Sample Analysis

Samples for total phosphate and total silicate were measured according to Grasshoff et al. (2009), using a Skalar San Plus auto-analyzer (Skalar Analytical B.V., Breda, the Netherlands). The TA was measured by open-cell titration (Dickson et al., 2007) using an AS-ALK2 titrator (Apollo SciTech, Newark, USA). DIC was measured using an AS-C3 analyzer (Apollo SciTech, Newark, USA), based on the infrared determination of the CO_2 in air resulting of the complete outgassing of the DIC after acidification of seawater with phosphoric acid. Both TA and DIC instruments were calibrated every measurement day with Certified Reference Material (CRM) (A. Dickson, Scripps Institution of Oceanography, La Jolla, USA). Based on recent inter-calibration effort by Andrew Dickson and Emily Bockmon (Scripps Institution of Oceanography, La Jolla), the accuracy (mean $\pm$ SD) of our TA and DIC measurements are 0.21 ± 1.93 and -3.34 ± 2.2 μmol/kg, respectively.

The CO_2 system was overdetermined (i.e., measurement of TA, DIC, and pH_T) in 36 discrete samples. The pH_T in this subset of discrete samples was measured by spectrophotometry in 10-cm pathlength quartz cuvettes following Dickson et al. (2007), using a custom-made Ocean Optics (Largo, USA) spectrometer system (Flame-S spectrometer, DH-mini light source) and m-Cresol purple purified dye obtained from Robert H. Byrne and Nora K. Douglas at the University of South Florida in St Petersburg. The samples and dye were maintained at 25 °C before measurement using a thermostatic bath. Based on measurements on CRM, we estimate the mean accuracy of the pH_T estimates at 0.004 units.

2.3. Data Analysis

The CO_2 system parameters were derived from the TA and DIC of the discrete samples, using the function "carb" of the R package Seacarb (Gattuso et al., 2019) with the first and second dissociation constants of the CO_2 system by Millero (2010) and the dissociation constants for HF and HSO_4^- of Dickson and Riley (1979) and Dickson (1990), respectively. The combined standard uncertainties in computed carbonate system variables were estimated by propagating instrumental error according to Orr et al. (2018) using the function "errors" of the R package Seacarb (Gattuso et al., 2018). The DIC and TA were normalized for salinity according to Friis et al. (2003), using the mean from all discrete samples and, as nonzero TA end-member, the intercept of the regression between TA and salinity for each ecosystem. The SeaFET pH data was converted to total scale using the temperature and salinity from the CTD. When not available (due to CTD malfunction), the temperature of the SeaFET thermistor was used, and the salinity was linearly interpolated over time. The pH_T was corrected using spectrophotometric pH_T measurements of a discrete sample collected after 15 days of initial deployments (Bresnahan et al., 2014; Kapsenberg & Hofmann, 2016; Rivest et al., 2016) using the Saltlantic Software SeaFETCom.

The mean ($\pm$ $SD)$ difference between the spectrophotometric pH_T in samples and the SeaFET measures are -0.001 ± 0.012, 0.003 ± 0.050 and 0.02 ± 0.20 in the coral reef, seagrass meadow and mangrove forest, respectively (Figure S1.). The precision and accuracy of the pH_T measurement in the coral reef and seagrass meadow were comparable to other studies in coastal ecosystems (McLaughlin et al., 2017). The precision and accuracy were, however, 1 order of magnitude lower in the mangrove forest waters, probably due to the extreme deployment conditions (high temperature and salinity, low water level with periods of emersions, exposure to sediment) and the high potential for large differences of the CO_2 system within a few cm between sampling point and sensor. In samples in which the CO_2 system was overdetermined ($n = 12, 11$ and 6 in the coral reef, seagrass meadow, and mangrove forest, respectively), the mean ($\pm SD$) difference between calculated pH_T from DIC and TA and pH_T spectrophotometric was 0.001 ± 0.015, -0.001 ± 0.014, and 0.028 ± 0.064 in the coral reef, seagrass meadow, and mangrove forest, respectively. These differences include instrumental error and a marginal contribution from organic alkalinity (Kuliński et al., 2014).

To compare between periods and ecosystems, we reduced the data by averaging the pH_T per hour of the day (1 to 24) over 15-day periods, based on the moon phases, to normalize for the influence of the semi-diurnal constituent of the tide and the neap to spring tide cycle. This allowed us to extract the influence of day-night cycles over tidal (and other non-light mediated parameters) influence. Thus, the spread of the value around
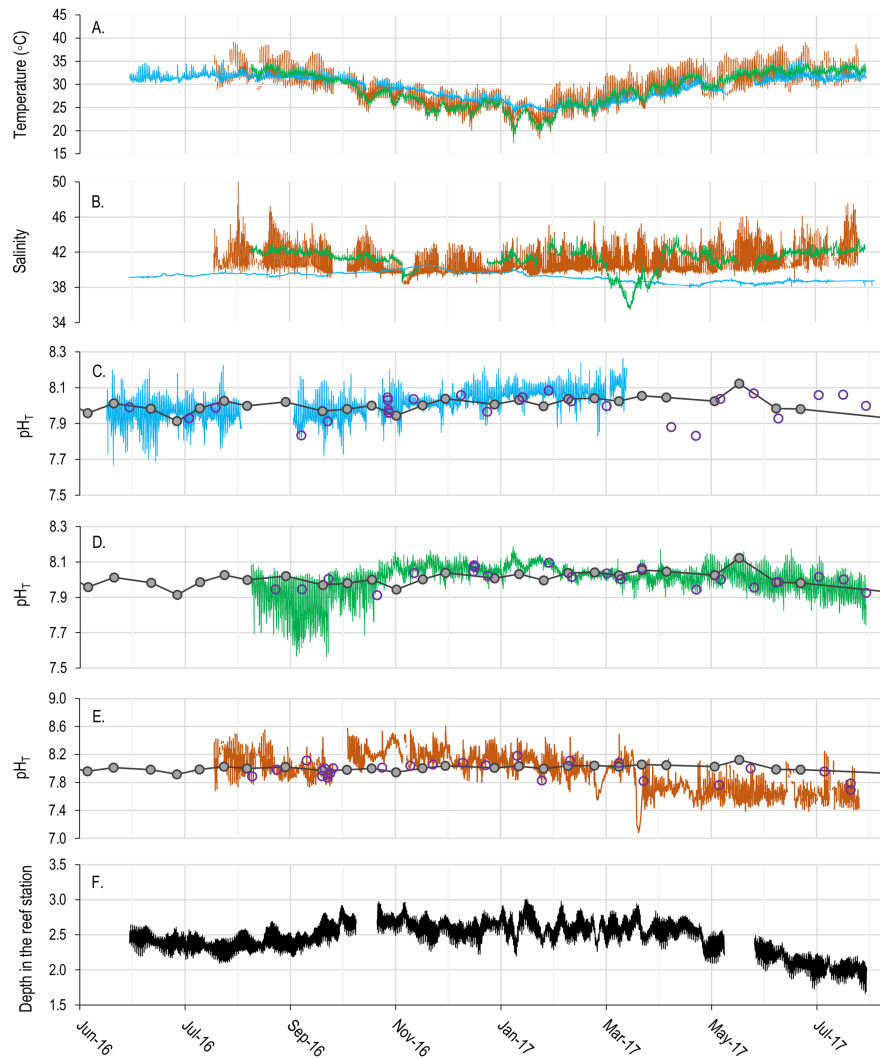
Figure 2. Time series of (a) temperature and (b) salinity in the coral reef (blue), seagrass meadow (green) and mangrove forest (brown) sites. pH_T (SeaFET) in the (c) coral reef, (d) seagrass meadow, and (e) mangrove forest sites. The plain dots are the pH_T calculated from discrete samples at the offshore reference site; the open dots are discrete measures of pH_T (spectrophotometric). (f) Water level in the coral reef site.

the hourly means, expressed as the mean absolute deviation (the average of the absolute deviations from mean; MAD), is indicative of the influence of tide and other fluctuations on pH_T.

$$\text{MAD} = \frac{1}{n} \times \sum_{h=1}^{n} \left| pH_T h - \overline{pH_T h} \right|$$

With n the number of days, $pH_T h$ the pH_T at hour h and $\overline{pH_T h}$ the mean pH_T for hour h for the n days.

3. Results and Discussion

3.1. Coral Reef

The mean ($\pm SD$) temperature during the sampling period in the coral reef site was 28.9 ± 3.6 °C with a mean diel variation ($\pm SD$) of 1.5 ± 0.4 °C (Figure 2a). The mean salinity in the coral reef was 39.3 ± 0.5 with 24h variations of 0.1 ± 0.9 (Figure 2b). The mean ($\pm SD$) pH_T during the complete recording period in the coral reef was 8.016 ± 0.077 (Figure 2c). The period with the minimum daily mean pH_T occurred between 27 June
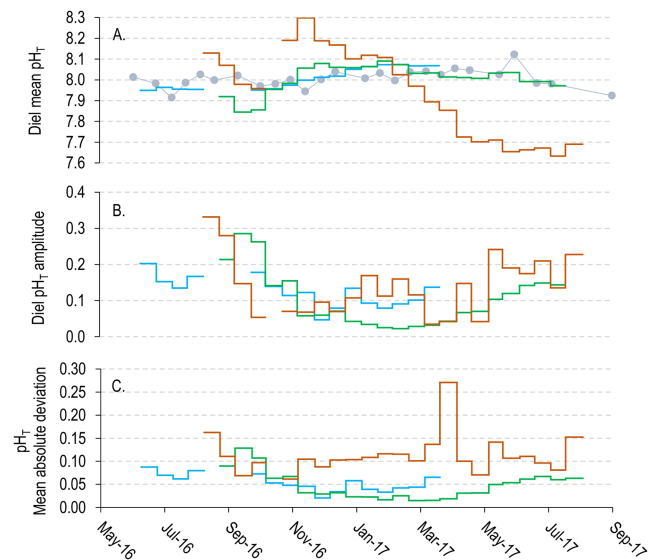
**Figure 3.** (a) Diel pH_T mean, (b) amplitude, and (c) mean absolute deviation (MAD) per 15 days periods in the coral reef (blue), seagrass meadow (green), and mangrove forest (brown) sites; the plain dots are the pH_T calculated from discrete samples at the offshore reference site.

2016 and 12 July 2016 with 7.949 increasing from summer to winter and peaking at 8.074 on the period from 18 February 2017 to 5 March 2017 (Figure 3a).

By comparison, the mean ($\pm SD$) pH_T (calculated from TA and DIC) in the offshore reference site during the whole measurement period was 8.006 ± 0.043 (95% confidence interval, CI, of 0.016; Figure 2c). The pH_T in the coral reef exceeded the 95% CI range of the offshore reference site for durations of 4.4 ± 2.5 and 4.9 ± 2.7 hr/day (mean $\pm SD$) in summer and autumn (dataset Saderne et al., 2019). Reciprocally, the pH_T in the coral reef was lower than the offshore 95% CI range during 15.8 ± 1.4 and 12.7 ± 7.14 hr/day in summer and autumn (Saderne et al., 2019). The situation reverses in winter, with a coral reef pH_T higher than the offshore 95%CI range 18.8 ± 6.3 hr/day, while lower for only 1.8 ± 3.5 hr/day (Saderne et al., 2019).

The pH_T daily maxima were around 14:00 MST (mean solar time) and the minima around 5:00 MST (Figure 4a). The maximum daily range of pH_T occurred in summer, during the first 15 days of measurement with 0.202. It narrowed through autumn winter to a minimum value of 0.046 during the first half of December, increasing thereafter (Figure 3b). A similar decrease in pH_T variations between summer and winter has been observed at Heron Island reef (Great Barrier Reef; Kline et al., 2015). However, the amplitudes of the diel variations in winter are lower than generally observed in other Indo-Pacific reef systems (Hofmann et al., 2011; Kline et al., 2015; Ohde & Woesik, 1999). Over the complete measurement period,
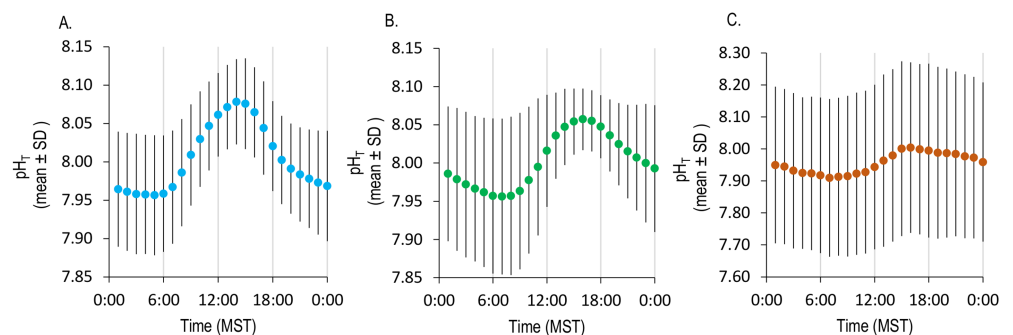

Figure 4. Hourly means ($\pm SD$) of pH_T for the entire measuring periods in (a) coral reef, (b) seagrass meadow, and (c) mangrove forest sites.
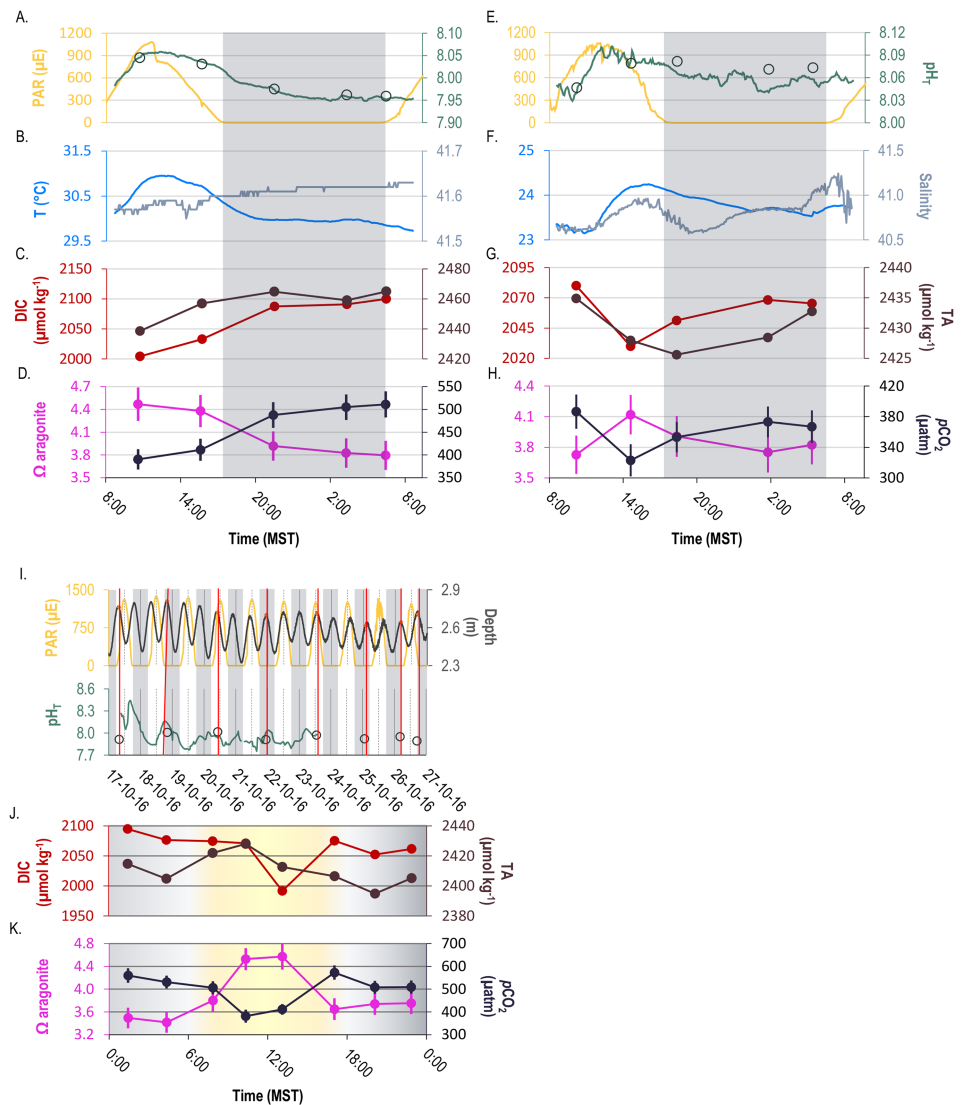
Figure 5. Diel cycle (24-hr sampling) of the CO_2 system in the (a–d) coral reef (November 2016), (e–h) seagrass meadow (January 2017) sites, and (i–k) artificial 24:00 series of pH_T and total alkalinity (TA) in the mangrove forest site at high tide (October 2016); samples were taken at high tide during a period of 10 days to determine light-mediated diel variation. (a, e, and i) pH_T continuous readings from SeaFET sensors; the open dots are spectrophotometric pH_T. The error bars are the propagated instrumental error on the CO_2 system parameters derived from total alkalinity and dissolved inorganic carbon (DIC).

the mean daily range of pH_T variation was 0.124 ± 0.04. As a comparison, mean diurnal changes of pH_T 0.12 ± 0.02 and 0.21 ± 0.02 were observed during a one-year survey in two coral reefs sites in Waimanalo (Oahu Island, Hawaii; Lantz et al., 2014). The MAD, representative of the influence of non-light mediated forcings on pH_T (i.e., principally tide), is <50% than the pH_T variations due to light (Figure 3c), following the same seasonal pattern as the daily range of pH_T variations. This seasonal dynamic of the MAD may be due to the seasonal variations of the water level in the Red Sea (Pugh & Abualnaja, 2015). Water level in the coral reef was lower by 0.23 cm on average in July–August 2016 compared to December–January (Figure 2f). The reduction of water depth over the coral reef may increase the influence of the diurnal tidal variations on seawater temperature and tend to amplify concentration of the TA and DIC, and therefore the pH_T variations, produced or released by the corals and other organisms.

A 24-hr survey of the complete CO_2 system was conducted on the 23–24th of November (Figures 5a–5d). The DICn and TAn were lower during day than during night of 94 μmol DIC/kg and 35 TA μmol/kg,
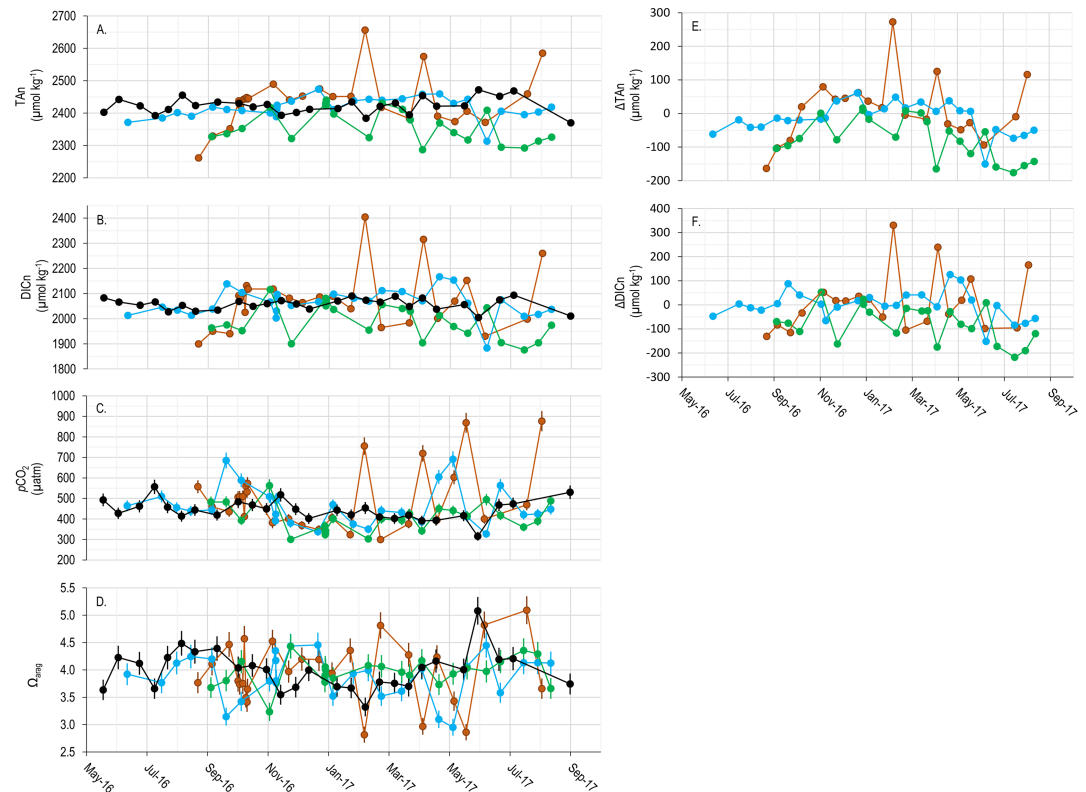
Figure 6. (a and b) Time series of measured TAn and DICn in the reef (light blue), seagrass meadow (green), mangrove forest (brown), and offshore reference (black) sites. (c and d) Calculated pCO_2 and Ω_{arag} in the three benthic ecosystems (e and f). TAn and DICn difference between benthic ecosystems and the offshore reference site. The error bars are the propagated instrumental error on the CO_2 system parameters derived from total alkalinity (TA) and dissolved inorganic carbon (DIC).

respectively. The calculated diel pCO_2 and Ω_{arag} decreased during that particular day by 121 µatm and 0.67 units, respectively. If considering all TA variation due to calcification, and a stoichiometric uptake of 2 µmol $TA \cdot kg^{-1}$ per µmol $DIC \cdot kg^{-1}$, we estimate that approximatively 18% of the diurnal DIC variation is due to calcification on that day. The diel variations of TA and DIC observed during the 24-hr sampling event in November 2016 compare with variations observed in Eilat in December (15 µmol TA/kg; Silverman et al., 2007). This 24h survey was conducted during a period of seasonally low diel variations, as revealed by the SeaFET mooring, and is therefore likely not representative of the diel variations in that location.

The mean ($\pm SD$) pCO_2, Ω_{arag}, DICn and TAn for the whole measurement period in the coral reef were 461 ± 39 µatm, 3.88 ± 0.43, 2061 ± 58 µmol DIC/kg, and 2415 ± 34 µmol TA/kg, respectively (Figures 6a–6d). We observed a decrease of DICn and TAn during the summer months compared to winter months. That reveals higher photosynthetic and calcification rates in summer, with 2032 ± 14 µmol DIC/kg and 2399 ± 10 µmol TA/kg, compared to 2086 ± 17 µmol DIC/kg and 2441 ± 20 µmol TA/kg in winter (mean ± 95%CI). We observed a similar trend for Ω_{arag} with 4.03 ± 0.14 in summer compared to 3.89 ± 0.34 (mean ± 95%CI) in winter (Figure 4d). The mean and variability of the seasonal pH_T, Ω_{arag}, and pCO_2 in our study coral reef are comparable to those reported for Media Luna Reef in Puerto Rico (Gray et al., 2012), The Florida Reef Tract (Manzello et al., 2012), Kaneohe Bay and Waimanalo in Hawaii (Drupp et al., 2013; CRIMP2 sampling site), the Bahamas (Yeakel et al., 2015) and Palmyra Island, Kingman Reef and Jarvis Island in the Line Islands (Price et al., 2012), that is, a pH_T between 7.9 and 8.1, Ω_{arag} between 3.5 and 4.5, and pCO_2 between 300 and 500 µatm (for review see Kline et al., 2015).

The slope of the regression between TAn and DICn is informative of the dominant metabolic processes in coral reef ecosystems (Andersson & Gledhill, 2013; Cyronak, Andersson, Langdon, et al., 2018; Lantz et al., 2014; Sippo et al., 2016). In Al-Fahal reef, the regression between TAn and DICn over the complete
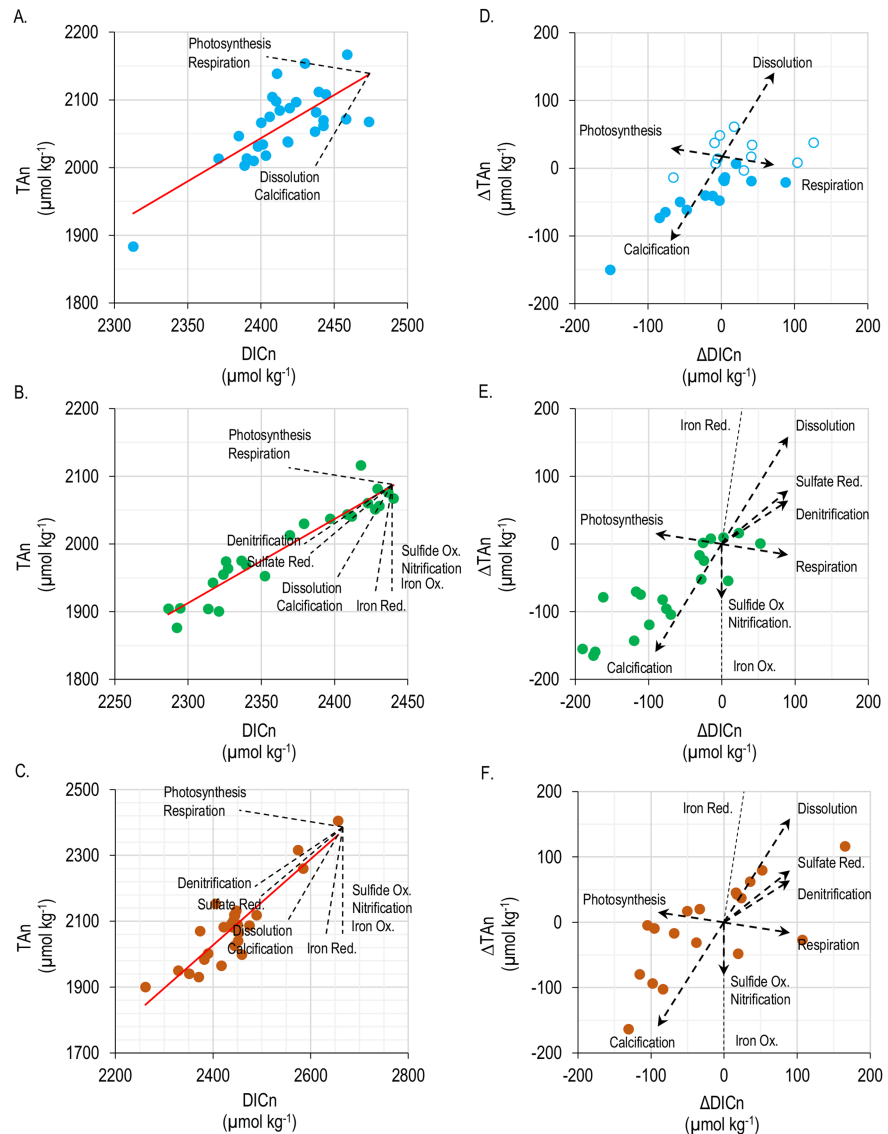
Figure 7. (a–c) TAn - DICn relationship in coral reef (blue), seagrass meadow (green), and mangrove forest (brown) sites. The dotted lines represent the stochiometric ratios of the major biogeochemical processes. Red solid line: linear regression. (d and e) TAn and DICn anomaly due to benthic ecosystems estimated as the difference with the offshore reference site and the coral reef, seagrass meadow, and mangrove forest sites. (d) The open dots are winter-spring data, and the plain dots are summer-autumn data in the coral reef site.

measurement period is statistically significant (F-statistic = 30.4, $p < 0.001$, $R^2 = 0.51$, n = 25), with a slope of 0.42 ($p < 0.001$; Figure 7a). This slope closely corresponds to the mean ($\pm$ *SD*) of the world coral reefs reported by Cyronak, Andersson, Langdon, et al. (2018) of 0.41 $\pm$ 0.18. The ratio between the TAn and DICn differences between the coral reef and the offshore reference site (Figures 6e and 6f and 7d) points at a dominance of heterotrophy and carbonate dissolution in winter-spring (November to May) and a prevalence of autotrophy and calcification in summer-autumn (June to November). This dynamic corroborates the findings of Roik et al. (2018) on the same coral reef during the period 2012-2015 using the ReefBudget approach (Perry et al., 2012). During the complete survey period, the coral reef was a sink of TA compared to open water with a mean difference of 15 μmol TA/kg, highlighting a minor dominance of calcification over dissolution.

In summary, our coral reef site does not display the high Ω_{arag} and low pH_T and pCO_2 that we could expect considering the high temperatures, salinities, and TA when compared to available data for other coral reefs

around the world. This could be explained by low DIC values relative to the TA in our study coral reef. The seasonal covariations of TA and DIC relative to open water tend to show higher autotrophy and calcification with increasing temperature from June to November. The current mean and variability of pCO_2 and pH recorded encompasses the OA projections for 2,100 in coral reefs by Hughes et al. (2017). This highlight the need to consider local means and variability of the CO_2 system in OA scenario and experiments.

3.2. Seagrass Meadow

The mean ($\pm SD$) temperature during the sampling period in the seagrass meadow site was 29.1 $\pm$ 2.6 °C (Figure 2a), with a mean diel variation ($\pm SD$) of 1.6 $\pm$ 0.9 °C. The mean salinity for the whole period was 41.2 $\pm$ 1.3, with 24-hr variations 0.8 $\pm$ 0.4 (Figure 2b). The mean salinity and temperature, as well as their diel variations, were higher in the seagrass meadow site compared to the coral reef site.

The mean ($\pm SD$) pH_T during the whole recording period in the seagrass meadow site was 8.00 $\pm$ 0.09 (Figure 2d), with a relatively narrow diel variability from maximum values (mean $\pm$ SD of 8.06 $\pm$ 0.04) at 16:00 to minimum values (7.96 $\pm$ 0.10) at 07:00 (Figure 4b). The minimum pH_T recorded occurred in late summer (7.84) and increased during autumn and winter to reach a maximum of 8.09 in February (Figure 3a). The diel variations followed the same seasonal trend, decreasing from 0.28 in September to 0.02 in February (Figure 3b). Over the measurement period, the MAD was 0.05 $\pm$ 0.04, compared to a mean diel variation of 0.10 $\pm$ 0.08 (mean $\pm$ SD; Figure 3c). So as in the coral reef site, the influence of light-mediated processes directly or indirectly caused by photosynthesis on the pH_T is approximately twice the influence of the tide and other physicochemical forcings.

The pH_T in the meadow during the summers 2016 and 2017 was below the 95% CI range in the offshore reference site (8.006 $\pm$ 0.016) 16.8 $\pm$ 5.1 and 15.1 $\pm$ 3.7 hr/day (mean $\pm$ SD), while higher only 2.9 $\pm$ 2.5 and 4.8 $\pm$ 4.7 hr/day (Saderne et al., 2019). The situation reversed in winter and spring, with a pH_T in the meadow above the pH_T in the offshore reference site for 21.5 $\pm$ 4.3 and 11.0 $\pm$ 5.8 hr/day, respectively, while 0.3 $\pm$ 0.8 and 4.6 $\pm$ 4.5 hr/day below (Saderne et al., 2019). In autumn, the duration periods during which the pH_T in the seagrass meadow is above and below the reference station pH_T 95% CI range are equivalent, 9.2 $\pm$ 9.7 and 10.9 $\pm$ 8.8 hr/day, respectively (Saderne et al., 2019).

There are only a few studies that document seasonal variations of the CO_2 system of seagrass meadows. Kapsenberg and Hofmann (2016) recorded pH_T (using SeaFET sensors) from 2012 to 2015 in a *Zostera pacifica* meadow in the California Channel Islands. They found a mean pH_T $\pm$ SD of 8.00 $\pm$ 0.06 over the whole measurement period, close to our value of 8.00 $\pm$ 0.09. However, seasonal patterns were very different. Kapsenberg and Hofmann (2016) found a maximum of mean pH_T occurring in June and declining through to October (from 8.06 $\pm$ 0.02 to 7.98 $\pm$ 0.02). Such seasonal trend was also observed in a *Thalassia testudinum* meadow in Florida (Eagle Harbor, St Joseph Bay; Challener et al., 2016). We found an opposite pattern in the Central Red Sea, with a pH_T minimum occurring in September and a maximum in February. However, this pattern is largely explained by the effect of the variation of temperature on pH. Normalized for 30 °C, the pH_T maximum is reached in June and the winter maximum disappears (Figure S2), highlighting an increased primary production. Kapsenberg & Hofmann (2016) observed a seasonal reduction of the diel variations from spring to autumn, with a minimum variation of 0.07 in November-December and a maximum variation of 0.2 in April, comparable to our observations.

We conducted a 24-hr survey on 11–12 January (Figures 5e–5h). We observed a modest diel variation of DICn and TAn on that day, 30 μmol DIC/kg and 25 μmol TA/kg. The minimum DICn occurred in the early evening while the minimum TAn occurred at mid-day. Both maximum values were reached at night (approximately 2:00 MST). The Ω_{arag} and pCO_2 variations mirrored each other, with values between Ω_{arag} between 3.7 and 4.1 and 385 and 326 μatm. These variations are quite modest compared to documented diel variations in seagrass meadows, often exceeding 100 μatm (e.g., Smith, 1981: Western Australia; Yates et al., 2007: Tampa and Florida Bay, Jiang et al., 2011: Taiwan, Challener et al., 2016: St Joseph Bay). However, the sampling was made during the period of the year when the amplitudes of variations are the minimum, as revealed by the pH_T series.

Over the whole measurement period, the means ($\pm SD$) DICn, TAn, pCO_2 and Ω_{arag} were 1986 $\pm$ 68 μmol DIC/kg, 2352 $\pm$ 49 μmol TA/kg, 411 $\pm$ 66 μatm, and 4.0 $\pm$ 0.3, respectively (Figures 6a–6d). The difference

of DICn and TAn between the offshore reference site and the seagrass meadow site were of -67 ± 70 μmol/kg and -63 ± 65 μmol/kg (mean $\pm$ SD; Figures 6e and 6f and 7b–7e), suggesting that the seagrass meadow is a sink for DIC and TA. We observed higher DICn and TAn in winter than summer, with means ($\pm$95%CI) of 2038 ± 43 μmol DIC/kg and 2401 ± 39 μmol TA/kg in winter compared to 1925 ± 37 μmol DIC/kg and 2311 ± 15 μmol TA/kg in summer. The mean pCO_2 was close to global atmospheric values (406 ppm in May 2017, NOAA-ESRL), varying from a seasonal minimum of 362 ± 37 μatm (mean $\pm$95% CI) in winter to a maximum of 427 ± 50 μatm in autumn. This seasonal difference is mainly due to the seasonal variation of temperature. Normalized for temperature (T = 30 °C), the calculated mean ($\pm$95%CI) pCO_2 are lower in summer than in winter, with 379 ± 48 μatm and 452 ± 26 μatm. These seasonal variations are of lesser amplitudes than observations made in *Thalassia testudinum* meadows in Florida (Eagle Harbor, St Joseph Bay; DICn: 330 μmol/kg, TAn: 220 μmol/kg, pCO_2: 430 μatm; Challener et al., 2016), but comparable to observations made in Mediterranean *Posidonia oceanica* meadows (Calvi, Corsica; DIC: 100 μmol/kg, TA: 50 μmol/kg; Frankignoulle & Bouquegneau, 1990).

3.3. Mangrove Forest

The mangrove forest site experienced comparable mean temperature and salinity as the coral reef site, but with more pronounced diel variations. The mean ($\pm$SD) temperature during the sampling period in the mangrove was 28.5 ± 3.5 °C (Figure 2a), with a mean diel variation ($\pm$SD) of 5.2 ± 1.6 °C. The mean salinity in the mangrove was 39.6 ± 0.9, with a mean diel variation of 3.8 ± 1.7 (Figure 2b).

The mean ($\pm$SD) pH_T during the entire study period in the mangrove forest was 7.95 ± 0.26 (Figure 2e), with a steady decrease of pH_T from 21 November 2016 (8.30) to 30 July 2017 (7.63; Figure 3a). The mean diel variations for the entire measurement period was 0.14 ± 0.08 with maximum pH_T at 16:00 (8.00 ± 0.27) and minimum pH_T at 7:00 (7.91 ± 0.25; Figure 4c). The diel variations increased from winter to summer months, with means (95% CI) of 0.110 ± 0.001 compared to 0.226 ± 0.002 (Figure 3b). The mean ($\pm$ SD) MAD over the whole measurement period was 0.11 ± 0.09, comparable to the mean diel variations (0.14 ± 0.08; Figure 3c), indicating that non-light mediated forcing, principally tides, have comparable influence on the CO_2 system than autotrophy.

The pH_T in the mangrove was higher than the offshore reference site 95% CI range for 7.6 ± 3.7, 14.8 ± 9.5, and 14.7 ± 8.4 hr/day in summer 2016, autumn, and winter, respectively, while lesser for 2.8 ± 3.6, 4.1 ± 6.2 hr/day and 6.6 ± 7.7 hr/day during those same seasons (Saderne et al., 2019). It reverses in spring and summer 2017, with lower pH_T than the offshore reference site 95% CI range most of the days, 17.4 ± 8.2 and 13.3 ± 5.9 hr/day (mean $\pm$ SD), respectively (Saderne et al., 2019). The pH_T in the mangrove forest was higher than the offshore reference site only 3.1 ± 6.6 hr/day and 0.2 ± 0.8 hr/day on average ($\pm$SD) in spring and summer 2017 (Saderne et al., 2019).

Part or all parameters of the CO_2 system of mangrove forest waters have been characterized in several studies (e.g., Borges et al., 2003; Bouillon et al., 2007; Call et al., 2015; Camp et al., 2016; Ray et al., 2018; Rosentreter et al., 2018; Sippo et al., 2016; Yates et al., 2014), but, to our knowledge, this is the first study to report a year-round survey of the CO_2 system of mangrove forest waters. All studies are pointing at large day-night and tidal variations of the CO_2 system, with pCO_2 variations of several thousand μatm and pH variations of more than one unit (e.g., Bouillon et al., 2007; Rosentreter et al., 2018; Sippo et al., 2016). As an example, daily mean pH of 6.30 to 6.91 with diel variations up to 1.12 were found in Queensland (Australia) mangrove systems with salinities above 30 (Rosentreter et al., 2018). Our survey shows a similar pattern, with diel and tidal variations of the pH of similar amplitude. Similarly, the decrease of the mean pH from winter to summer could be linked to the low water stage during summer months in the Red Sea due to seasonal variations in wind regimes and water mass exchanges with the Indian Ocean (Pugh & Abualnaja, 2015).

The mean ($\pm$ SD) yearly DICn and TAn in mangrove were 2069 ± 132 μmol DIC/kg and 2.438 ± 91 μmol TA/kg (Figures 6a and 6b), representing differences with the offshore reference station of 17 ± 96 μmol DIC/kg and 14 ± 123 μmol TA/kg (Figures 6e and 6f and 7c and 7d). Thus, we did not find systematic differences between mangrove forest and offshore water DIC and TA. The mean ($\pm$ SD) pCO_2 and Ω_{arag} in the mangrove were 493 ± 178 μatm and 4.1 ± 0.6 (Figures 6c and 6d).

To isolate the influence of light from the influence of tidal stage on the CO_2 system variations and therefore obtain a better picture of the processes driving TA and DIC, we performed extra samplings at high tide at different hours of the day- night cycle throughout 10 days (Figures 5i–5k). We observed a day - night cycle of DIC and TA, centered on noon. The DICn amplitude was 100 μmol DIC/kg and TAn 48 μmol TA/kg. It resulted in maximum amplitude of Ω_{arag} and pCO_2 of 0.38 and 191 μatm (ranging from 3.4 to 3.8 and 380 to 573 μatm). We found a relative increase of TAn and decrease of DICn at daytime (compared to nighttime), causing an increase of Ω_{arag}. This sampling effort highlights the circadicity of TA and DIC and call for more in-depth studies on the short time scale variability of the CO_2 system in mangrove forests.

3.4. Drivers of the CO_2 System in the Mangrove and Seagrass Ecosystems

The variations of the CO_2 systems in mangrove forest and seagrass meadows are the result of numerous and complex metabolic processes of the plant themselves, as well as of the associated flora, fauna, and the sediment. These metabolic processes are driven by physical and chemical variables, such as light, tides, temperature or salinity. Partitioning between the causes of the observed CO_2 system variations is difficult. Generally, the most important processes at play are primary production (new and recycled), respiration, calcification and red-ox reactions in the sediment involving various aerobic and anaerobic processes. The plants indirectly drive these reactions through the injection of O_2 and organic matter into the sediment.

Mangrove forests and seagrass meadows (and saltmarshes) are often highlighted for their high burial rates and sequestration of organic matter in their sediments and have therefore been coined "blue carbon" ecosystems. In those sediments, the labile part of the buried organic matter follows a sequence of degradation and remineralization from surface to depth. In surface oxic sediments, the organic matter is degraded through aerobic respiration, generating CO_2 (DIC). Below O_2 penetration depth in the sediment, the degradation of organic matter occurs by hydrolysis and fermentation though a cascade of reductive processes, the final reduced metabolite produced at depth being methane (Middelburg & Levin, 2009). These reduced metabolites are however being re-oxidized in surface sediments, consuming therefore O_2. In that regards, the sulfate reduction - sulfide oxidation cycle is predominant, due to the high amount of sulfate in seawater. Sulfide is phytotoxic and marine angiosperms actively supply O_2 to the sediment through their roots and rhizome system to prevent the accumulation of this reduced compound (Lamers et al., 2013). Doing so, marine angiosperms strongly influence the redox status of their sediment, and therefore the emissions of TA and DIC to the water column, causing variations of the CO_2 system. Thus, mangrove and seagrass sediments have specific metabolic activities, different from non-vegetated sediment, and are therefore an active component of the ecosystem.

The stoichiometry of the relationship between DIC and TA informs of the dominant processes driving the CO_2 system (Krumins et al., 2013; Sippo et al., 2016). In both seagrass meadows and mangrove forests, the TAn - DICn regression were highly significant (F-statistic = 145, $n =$, $p < 0.001$, $R^2 = 0.86$, $n = 21$ and $F = 79$, $p < 0.001$, $R^2 = 0.76$, $n = 20$, respectively) with a similar value for the slopes of 0.65 ± 0.05 and 0.65 ± 0.07, respectively (both $p < 0.001$; Figures 7b and 7c). These slopes are close to the stoichiometry of the anaerobic processes of denitrification and sulfate reduction. The TAn-DICn relationship in our mangrove forest and seagrass meadow corresponds to previous observations in seagrass and mangroves (Challener et al., 2016; Sippo et al., 2016).

Corroborating the slopes, Garcias-Bonet et al. (2018) demonstrated very high rates of net denitrification in our study meadow, 1 to 6-fold higher than in seagrass meadows elsewhere. We do not have information regarding the balance between sulfate reduction-sulfite oxidation at our mangrove forest and seagrass meadow sites. However, there are arguments in the literature against net sulfate reduction in carbonate sediments containing low iron (Burdige et al., 2010; Holmer et al., 2005; Hu & Burdige, 2007; Krumins et al., 2013), such as in our seagrass meadow and mangrove forest sites (Almahasheer, Duarte, & Irigoien, 2016; Anton et al., 2018; Saderne et al., 2018).

We observed a negative anomaly of DIC and TA in the seagrass meadow relative to the offshore site (Figure 7e). This seems to be in contradiction with net denitrification as a driver of the CO_2 system, as this process is source of TA. Rather, that comparison seems to point at the dominance of photosynthesis, calcification and oxidative reactions. Photosynthesis seems to be an obvious driver of the DIC depletion observed in the meadow. Primary production has a slight effect on TA, which depends on

the source of nitrogen used. New primary production, based on nitrate, produces 0.16 unit of TA per DIC produced while recycled primary production, based on Ammonium, consumes about 0.14 unit of TA per DIC produced (Brewer & Goldman, 1976; Goldman & Brewer, 1980). Biologically mediated calcification (biomineralization) in the meadow as a driver of the negative anomaly of DIC and TA does not appear obvious. Leaves of *E. acoroides* at our survey site are free of calcifying epibionts and we could only observe the presence in the meadow of sparse corals of the genus Porites as major benthic calcifiers. Chemogenic precipitation of $CaCO_3$ can occur in low iron, carbonate sediments of tropical seagrass meadows (Burdige & Zimmerman, 2002; Hu & Burdige, 2007; Ku et al., 1999). Besides calcification, the two other main TA sinks in sediments are sulfide and reduced iron burial (Krumins et al., 2013). However, the lack of iron in the Red Sea sediment preclude reduced iron burial as an important sink of TA in our ecosystems.

In the mangrove forest site, we did not find systematic differences between the offshore reference site and the mangrove forest site throughout the year (Figure 7f). A strong variability of export rates of TA and DIC from Australian mangroves have been found by Sippo et al. (2016), ranging from -1 to 116 mmol $TA \cdot m^{-2} \cdot day^{-1}$ and -97 to 85 mmol $DIC \cdot m^{-2} \cdot day^{-1}$. To have comparable samples all along the year, we only sampled at high tide and around noon, corresponding to an alignment of the two astronomic cycles only occurring for a few days every two weeks. Noon corresponds to the lowest DIC of the day and intermediate TA value and the high tide corresponds to the maximum dilution potential (Cyronak, Andersson, D'Angelo, et al., 2018). As shown by the pH variability, there is a large variation of the CO_2 system due to the tide and the time of the day. A very different time series of TA and DIC could have resulted from sampling along a different time and tidal stage.

Our survey sites - the coral reef, seagrass meadow, mangrove forest, and the offshore reference site - are not isolated from each other but are on a continuum from open sea to nearshore. Depending on the direction and strength of the currents and residency time of water, the CO_2 system measured in one ecosystem will partially depend on the processes that affected the water masses upstream. Thus, for example, the CO_2 system anomaly relative to offshore water observed at the seagrass site in a coastal lagoon could be partially due to calcification by reefs upstream. Quantifying the exports of TA and DIC by benthic ecosystems requires hydrological and bathymetrical data and models we do not have available now. Quantifying those TA and DIC exchanges between coastal ecosystems could inform of how blue carbon ecosystems could contribute to the growth of downstream reefs (Sippo et al., 2016).

4. Conclusions

In the coral reef, we observed a summer decrease of TA and DIC, possibly attributable to an increase of calcification and photosynthesis rates. The CO_2 system levels and variability in the coral reef are comparable to other reefs around the world, as revealed by the TA to DIC relationship and despite the higher salinity and warmer temperature. Our site already experiences pH and pCO_2 within the probable acidification scenario in coral reefs for the century described in Hughes et al., (2017). This survey proves the relevance of taking into account the local conditions of the CO_2 system to design acidification scenarios.

We observed a negative anomaly of TA and DIC in the seagrass *E. acoroides* meadow relative to offshore water. The mangrove forest showed the largest variation in pH, due to day-night and tidal cycles. Higher-frequency studies at different spatial scales, made possible by emerging new technologies (e.g., TA sensor in Briggs et al., 2017), are needed to fully characterize the ecosystems CO_2 system and determine their role as a source or sink of TA and DIC. Hydrological data and models, absent in our study, are needed to quantify the actual contribution of nearshore vegetated ecosystems to the CO_2 system in reefs and therefore answer the question of the benefits of vegetated ecosystems to coral reef calcification in a context of ocean acidification.

References

Almahasheer, H., Aljowair, A., Duarte, C. M., & Irigoien, X. (2016). Decadal stability of Red Sea mangroves. *Estuarine, Coastal and Shelf Science*, *169*, 164–172. https://doi.org/10.1016/j.ecss.2015.11.027

Almahasheer, H., Duarte, C. M., & Irigoien, X. (2016). Nutrient limitation in central Red Sea mangroves. *Frontiers in Marine Science*, *3*. https://doi.org/10.3389/fmars.2016.00271

Andersson, A. J., & Gledhill, D. (2013). Ocean acidification and coral reefs: effects on breakdown, dissolution, and net ecosystem calcification. *Annual Review of Marine Science*, *5*(1), 321–348. https://doi.org/10.1146/annurev-marine-121211-172241

Andersson, A. J., & MacKenzie, F. T. (2012). Revisiting four scientific debates in ocean acidification research. *Biogeosciences*, *9*(3), 893–905. https://doi.org/10.5194/bg-9-893-2012

Anton, A., Hendriks, I. E., Marbà, N., Krause-Jensen, D., Garcias-Bonet, N., & Duarte, C. M. (2018). Iron deficiency in seagrasses and macroalgae in the Red Sea is unrelated to latitude and physiological performance. *Frontiers in Marine Science*, *5*(March), 1–14. https://doi.org/10.3389/fmars.2018.00074

Borges, A. V., Djenidi, S., Lacroix, G., Theate, J., & Delille, B. F. M. (2003). Atmospheric CO_2 flux from mangrove surrounding waters. *Geophysical Research Letters*, *30*(11), 1558. https://doi.org/10.1029/2003GL017143

Bouillon, S., Middelburg, J. J., Dehairs, F., Borges, A. V., Abril, G., Flindt, M. R., et al. (2007). Importance of intertidal sediment processes and porewater exchange on the water column biogeochemistry in a pristine mangrove creek (Ras Dege, Tanzania). *Biogeosciences*, *4*(3), 311–322. https://doi.org/10.5194/bg-4-311-2007

Bresnahan, P. J., Martz, T. R., Takeshita, Y., Johnson, K. S., & LaShomb, M. (2014). Best practices for autonomous measurement of seawater pH with the Honeywell Durafet. *Methods in Oceanography*, *9*(October), 44–60. https://doi.org/10.1016/j.mio.2014.08.003

Brewer, P. G., & Goldman, J. C. (1976). Alkalinity changes generated by phytoplankton growth. *Limnology and Oceanography*, *21*(1), 108–117. https://doi.org/10.4319/lo.1976.21.1.0108

Briggs, E. M., Sandoval, S., Erten, A., Takeshita, Y., Kummel, A. C., & Martz, T. R. (2017). Solid State Sensor for Simultaneous Measurement of Total Alkalinity and pH of Seawater. *ACS Sensors*, *2*(9), 1302–1309. https://doi.org/10.1021/acssensors.7b00305

Burdige, D. J., Hu, X., & Zimmerman, R. C. (2010). The widespread occurrence of coupled carbonate dissolution/reprecipitation in surface sediments on the Bahamas Bank. *American Journal of Science*, *310*(6), 492–521. https://doi.org/10.2475/06.2010.03

Burdige, D. J., & Zimmerman, R. C. (2002). Impact of sea grass density on carbonate dissolution in Bahamian sediments. *Limnology and Oceanography*, *47*(6), 1751–1763. https://doi.org/10.4319/lo.2002.47.6.1751

Call, M., Maher, D. T., Santos, I. R., Ruiz-Halpern, S., Mangion, P., Sanders, C. J., et al. (2015). Spatial and temporal variability of carbon dioxide and methane fluxes over semi-diurnal and spring-neap-spring timescales in a mangrove creek. *Geochimica et Cosmochimica Acta*, *150*, 211–225. https://doi.org/10.1016/j.gca.2014.11.023

Camp, E. F., Schoepf, V., Mumby, P. J., & Suggett, D. J. (2018). The future of coral reefs subject to rapid climate change: lessons from natural extreme environments. *Frontiers in Marine Science*, *5*(February), 4. https://doi.org/10.3389/fmars.2018.00433

Camp, E. F., Suggett, D. J., Gendron, G., Jompa, J., Manfrino, C., & Smith, D. J. (2016). Mangrove and seagrass beds provide different biogeochemical services for corals threatened by climate change. *Frontiers in Marine Science*, *3*(April), 1–16. https://doi.org/10.3389/fmars.2016.00052

Chaidez, V., Dreano, D., Agusti, S., Duarte, C. M., & Hoteit, I. (2017). Decadal trends in Red Sea maximum surface temperature. *Scientific Reports*, *7*(1), 1–8. https://doi.org/10.1038/s41598-017-08146-z

Challener, R. C., Robbins, L. L., & Mcclintock, J. B. (2016). Variability of the carbonate chemistry in a shallow, seagrass-dominated ecosystem: Implications for ocean acidification experiments. *Marine and Freshwater Research*, *67*(2), 163–172. https://doi.org/10.1071/MF14219

Cyronak, T., Andersson, A. J., D'Angelo, S., Bresnahan, P., Davidson, C., Griffin, A., et al. (2018). Short-term spatial and temporal carbonate chemistry variability in two contrasting seagrass meadows: implications for pH buffering capacities. *Estuaries and Coasts*, *41*(5), 1282–1296. https://doi.org/10.1007/s12237-017-0356-5

Cyronak, T., Andersson, A. J., Langdon, C., Albright, R., Bates, N. R., Caldeira, K., et al. (2018). Taking the metabolic pulse of the world's coral reefs. *PLoS ONE*, *13*(1), 1–17. https://doi.org/10.1371/journal.pone.0190872

Dickson, A. G. (1990). Standard potential of the reaction: AgCl(s) + 1/2H$_2$(g) = Ag(s) + HCl (aq), and the standard acidity constant of the ion HSO$_4^-$ in synthetic sea water from 273.15 to 318.15 K. *The Journal of Chemical Thermodynamics*, *22*(2), 113–127. https://doi.org/10.1016/0021-9614(90)90074-Z

Dickson, A. G., & Riley, P. J. (1979). The estimation of acid dissociation constants in seawater media from potentiometric titrations with strong base. II. The dissociation of phosphoric acid. *Marine Chemistry*, *7*, 101–109.

Dickson, A. G., Sabine, C. L., & R, C. J. (2007). *Guide to best practices for ocean CO_2 measurements. PICES Special Publication*, (Vol. 3). Sidney, British Columbia: North Pacific Marine Science Organization. https://doi.org/10.1159/000331784

Drupp, P. S., De Carlo, E. H., Mackenzie, F. T., Sabine, C. L., Feely, R. A., & Shamberger, K. E. (2013). Comparison of CO_2 dynamics and air-sea gas exchange in differing tropical reef environments. *Aquatic Geochemistry*, *19*(5–6), 371–397. https://doi.org/10.1007/s10498-013-9214-7

Duarte, C. M., Hendriks, I. E., Moore, T. S., Olsen, Y. S., Steckbauer, A., Ramajo, L., et al. (2013). Is Ocean Acidification an Open-Ocean Syndrome? Understanding Anthropogenic Impacts on Seawater pH. *Estuaries and Coasts*, *36*(2), 221–236. https://doi.org/10.1007/s12237-013-9594-3

Fassbender, A. J., Sabine, C. L., & Feifel, K. M. (2016). Consideration of coastal carbonate chemistry in understanding biological calcification. *Geophysical Research Letters*, *43*, 4467–4476. https://doi.org/10.1002/2016GL068860

Frankignoulle, M., & Bouquegneau, J. M. (1990). Daily and yearly variations of total inorganic carbon in a productive coastal area. *Estuarine, Coastal and Shelf Science*, *30*(1), 79–89. https://doi.org/10.1016/0272-7714(90)90078-6

Friis, K., Körtzinger, A., & Wallace, D. W. R. (2003). The salinity normalization of marine inorganic carbon chemistry data. *Geophysical Research Letters*, *30*(2), 1085. https://doi.org/10.1029/2002GL015898

Garcias-Bonet, N., Fusi, M., Ali, M., Shaw, D. R., Saikaly, P. E., Daffonchio, D., & Duarte, C. M. (2018). High denitrification and anaerobic ammonium oxidation contributes to net nitrogen loss in a seagrass ecosystem in the central Red Sea. *Biogeosciences*, *15*(23), 7333–7346. https://doi.org/10.5194/bg-15-7333-2018

Gattuso, J.-P., Epitalon, J.-M., & Lavigne, H. (2019). seacarb: Seawater Carbonate Chemistry. R package version 3.2.12. Software. Retrieved from http://scholar.google.com/scholar?hl=en&btnG=Search&q=intitle:seacarb:+seawater+carbonate+chemistry+with+R.+R+package+version+2.3#0

Goldman, J. C., & Brewer, P. G. (1980). Effect of nitrogen source and growth rate on phytoplankton-mediated changes in alkalinity. *Limnology and Oceanography*, *25*(2), 352–357. https://doi.org/10.4319/lo.1980.25.2.0352

Grasshoff, K., Ehrhardt, M., & Kremling, K. (2009). In K. Grasshoff, K. Kremling, & M. Ehrhardt (Eds.), *Methods of seawater analysis*. John Wiley & Sons. https://doi.org/10.1002/9783527613984

Gray, S. E. C., DeGrandpre, M. D., Langdon, C., & Corredor, J. E. (2012). Short-term and seasonal pH. *Global Biogeochemical Cycles*, *26*, GB3012. https://doi.org/10.1029/2011GB004114

Harvey, B. P., Gwynn-Jones, D., & Moore, P. J. (2013). Meta-analysis reveals complex marine biological responses to the interactive effects of ocean acidification and warming. *Ecology and Evolution*, *3*(4), 1016–1030. https://doi.org/10.1002/ece3.516

Hofmann, G. E., Smith, J. E., Johnson, K. S., Send, U., Levin, L. A., Micheli, F., et al. (2011). High-frequency dynamics of ocean pH: A multi-ecosystem comparison. *PLoS ONE*, *6*(12), e28983. https://doi.org/10.1371/journal.pone.0028983

Holmer, M., Duarte, C. M., & Marbá, N. (2005). Iron additions reduce sulfate reduction rates and improve seagrass growth on organic-enriched carbonate sediments. *Ecosystems*, *8*(6), 721–730. https://doi.org/10.1007/s10021-003-0180-6

Hu, X., & Burdige, D. J. (2007). Enriched stable carbon isotopes in the pore waters of carbonate sediments dominated by seagrasses: Evidence for coupled carbonate dissolution and reprecipitation. *Geochimica et Cosmochimica Acta*, *71*(1), 129–144. https://doi.org/10.1016/j.gca.2006.08.043

Hughes, T. P., Anderson, K. D., Connolly, S. R., Heron, S. F., Kerry, J. T., Lough, J. M., et al. (2018). Spatial and temporal patterns of mass bleaching of corals in the Anthropocene. *Science*, *359*(6371), 80–83. https://doi.org/10.1126/science.aan8048

Hughes, T. P., Barnes, M. L., Bellwood, D. R., Cinner, J. E., Cumming, G. S., Jackson, J. B. C., et al. (2017). Coral reefs in the Anthropocene. *Nature*, *546*(7656), 82–90. https://doi.org/10.1038/nature22901

Hunter, K. A. (1998). The temperature dependence of pH in surface seawater. *Deep-Sea Research Part I: Oceanographic Research Papers*, *45*(11), 1919–1930. https://doi.org/10.1016/S0967-0637(98)00047-8

Jiang, Z.-P. J. C. H., Dai, M., Kao, S. J., Hydes, D. J., Chou, W.-C., & Jan, S. (2011). Short-term dynamics of oxygen and carbon in productive nearshore shallow seawater systems off Taiwan: Observations and modeling. *Limnology and Oceanography*, *56*(5), 1832–1849. https://doi.org/10.4319/lo.2011.56.5.0000

Kapsenberg, L., & Hofmann, G. E. (2016). Ocean pH time-series and drivers of variability along the northern Channel Islands, California, USA. *Limnology and Oceanography*, *61*(3), 953–968. https://doi.org/10.1002/lno.10264

Kenworthy, W. J., Wyllie-Echeverria, S., Coles, R. G., Pergent, G., & Pergent-Martini, C. (2006). Seagrass Conservation Biology: An Interdisciplinary Science for Protection of the Seagrass Biome. In *Seagrasses: biology, ecology and conservation*, (pp. 595–623). Dordrecht: Springer Netherlands. https://doi.org/10.1007/978-1-4020-2983-7_25

Kline, D. I., Teneva, L., Hauri, C., Schneider, K., Miard, T., Chai, A., et al. (2015). Six month in situ high-resolution carbonate chemistry and temperature study on a coral reef flat reveals asynchronous pH and temperature anomalies. *PLoS ONE*, *10*(6), e0127648–e0127626. https://doi.org/10.1371/journal.pone.0127648

Krumins, V., Gehlen, M., Arndt, S., Van Cappellen, P., & Regnier, P. (2013). Dissolved inorganic carbon and alkalinity fluxes from coastal marine sediments: Model estimates for different shelf environments and sensitivity to global change. *Biogeosciences*, *10*(1), 371–398. https://doi.org/10.5194/bg-10-371-2013

Ku, T. C. W., Walter, L. M., Coleman, M. L., Blake, R. E., & Martini, A. M. (1999). Coupling between sulfur recycling and syndepositional carbonate dissolution: Evidence from oxygen and sulfur isotope composition of pore water sulfate, South Florida Platform, U.S.A. *Geochimica et Cosmochimica Acta*, *63*(17), 2529–2546. https://doi.org/10.1016/S0016-7037(99)00115-5

Kuliński, K., Schneider, B., Hammer, K., Machulik, U., & Schulz-Bull, D. (2014). The influence of dissolved organic matter on the acid-base system of the Baltic Sea. *Journal of Marine Systems*, *132*, 106–115. https://doi.org/10.1016/j.jmarsys.2014.01.011

Lamers, L. P. M., Govers, L. L., Janssen, I. C. J. M., Geurts, J. J. M., van der Welle, M. E. W., van Katwijk, M. M., et al. (2013). Sulfide as a soil phytotoxin—A review. *Frontiers in Plant Science*, *4*(July), 268. https://doi.org/10.3389/fpls.2013.00268

Lantz, C. A., Atkinson, M. J., Winn, C. W., & Kahng, S. E. (2014). Dissolved inorganic carbon and total alkalinity of a Hawaiian fringing reef: Chemical techniques for monitoring the effects of ocean acidification on coral reefs. *Coral Reefs*, *33*(1), 105–115. https://doi.org/10.1007/s00338-013-1082-5

Manzello, D. P., Enochs, I. C., Melo, N., Gledhill, D. K., & Johns, E. M. (2012). Ocean acidification refugia of the Florida reef tract. *PLoS ONE*, *7*(7), e41715. https://doi.org/10.1371/journal.pone.0041715

Martz, T. R., Connery, J. G., & Johnson, K. S. (2010). Testing the Honeywell Durafet® for seawater pH applications. *Limnology and Oceanography: Methods*, *8*(May), 172–184. https://doi.org/10.4319/lom.2010.8.172

McLaughlin, K., Dickson, A., Weisberg, S. B., Coale, K., Elrod, V., Hunter, C., et al. (2017). An evaluation of ISFET sensors for coastal pH monitoring applications. *Regional Studies in Marine Science*, *12*, 11–18. https://doi.org/10.1016/j.rsma.2017.02.008

Middelburg, J. J., & Levin, L. A. (2009). Coastal hypoxia and sediment biogeochemistry. *Biogeosciences*, *6*(7), 1273–1293. https://doi.org/10.5194/bg-6-1273-2009

Millero, F. J. (2010). Carbonate constants for estuarine waters. *Marine and Freshwater Research*, *61*(2), 139. https://doi.org/10.1071/MF09254

Monroe, A. A., Ziegler, M., Roik, A., Röthig, T., Hardenstine, R. S., Emms, M. A., et al. (2018). In situ observations of coral bleaching in the central Saudi Arabian Red Sea during the 2015/2016 global coral bleaching event. *PLoS ONE*, *13*(4), 1–13. https://doi.org/10.1371/journal.pone.0195814

Ohde, S., & Woesik, R. V. (1999). carbon dioxide flux and metabolic processes of a coral reef, Okinawa. *Bulletin of Marine Science*, *65*(2), 559–576.

Orr, J. C. (2011). Recent and future changes in ocean carbonate chemistry. *Ocean Acidification*, *2*, 41–66.

Orr, J. C., Epitalon, J. M., Dickson, A. G., & Gattuso, J. P. (2018). Routine uncertainty propagation for the marine carbon dioxide system. *Marine Chemistry*, *207*(June), 84–107. https://doi.org/10.1016/j.marchem.2018.10.006

Perry, C. T., Edinger, E. N., Kench, P. S., Murphy, G. N., Smithers, S. G., Steneck, R. S., & Mumby, P. J. (2012). Estimating rates of biologically driven coral reef framework production and erosion: A new census-based carbonate budget methodology and applications to the reefs of Bonaire. *Coral Reefs*, *31*(3), 853–868. https://doi.org/10.1007/s00338-012-0901-4

Price, N. N., Martz, T. R., Brainard, R. E., & Smith, J. E. (2012). Diel variability in seawater pH relates to calcification and benthic community structure on coral reefs. *PLoS ONE*, *7*(8), e43843. https://doi.org/10.1371/journal.pone.0043843

Pugh, D. T., & Abualnaja, Y. (2015). Sea-level changes. In *The Red Sea*, (pp. 317–328). Berlin Heidelberg: Springer. https://doi.org/10.1007/978-3-662-45201-1_18

Ray, R., Baum, A., Rixen, T., Gleixner, G., & Jana, T. K. (2018). Exportation of dissolved (inorganic and organic) and particulate carbon from mangroves and its implication to the carbon budget in the Indian Sundarbans. *Science of the Total Environment*, *621*, 535–547. https://doi.org/10.1016/j.scitotenv.2017.11.225

Rivest, E. B., Comeau, S., & Cornwall, C. E. (2017). The Role of Natural Variability in Shaping the Response of Coral Reef Organisms to Climate Change. *Current Climate Change Reports*, *3*(4), 271–281. https://doi.org/10.1007/s40641-017-0082-x

Rivest, E. B., O'Brien, M., Kapsenberg, L., Gotschalk, C. C., Blanchette, C. A., Hoshijima, U., & Hofmann, G. E. (2016). Beyond the benchtop and the benthos: Dataset management planning and design for time series of ocean carbonate chemistry associated with Durafet®-based pH sensors. *Ecological Informatics*, *36*, 209–220. https://doi.org/10.1016/j.ecoinf.2016.08.005

Roik, A., Röthig, T., Pogoreutz, C., Saderne, V., & Voolstra, C. R. (2018). Coral reef carbonate budgets and ecological drivers in the central Red Sea - A naturally high temperature and high total alkalinity environment. *Biogeosciences*, *15*(20), 6277–6296. https://doi.org/10.5194/bg-15-6277-2018

Rosentreter, J. A., Maher, D. T., Erler, D. V., Murray, R., & Eyre, B. D. (2018). Seasonal and temporal CO2 dynamics in three tropical mangrove creeks—A revision of global mangrove CO2 emissions. *Geochimica et Cosmochimica Acta*, *222*, 729–745. https://doi.org/10.1016/j.gca.2017.11.026

Saderne, V., Baldry, K., Anton, A., Agustí, S., & Duarte, C. M. (2019). Characterization of the CO_2 system in a coral reef, a seagrass meadow and a mangrove forest in the central Red Sea. *PANGAEA*. https://doi.org/10.1594/PANGAEA.906954

Saderne, V., Cusack, M., Almahasheer, H., Serrano, O., Masqué, P., Arias-Ortiz, A., et al. (2018). Accumulation of carbonates contributes to coastal vegetated ecosystems keeping pace with sea level rise in an arid region (Arabian Peninsula). *Journal of Geophysical Research: Biogeosciences*, *123*, 1498–1510. https://doi.org/10.1029/2017JG004288

Silverman, J., Lazar, B., & Erez, J. (2007). Effect of aragonite saturation, temperature, and nutrients on the community calcification rate of a coral reef. *Journal of Geophysical Research*, *112*, C05004. https://doi.org/10.1029/2006JC003770

Sippo, J. Z., Maher, D. T., Tait, D. R., Holloway, C., & Santos, I. R. (2016). Are mangroves drivers or buffers of coastal acidification? Insights from alkalinity and dissolved inorganic carbon export estimates across a latitudinal transect. *Global Biogeochemical Cycles*, *30*, 753–766. https://doi.org/10.1002/2015GB005324

Smith, S. V. (1981). Marine macrophytes as a global carbon sink. *Science*, *211*(4484), 838–840. https://doi.org/10.1126/science.211.4484.838

Takahashi, T., Sutherland, S. C., Chipman, D. W., Goddard, J. G., & Ho, C. (2014). Climatological distributions of pH, pCO$_2$, total CO$_2$, alkalinity, and CaCO$_3$ saturation in the global surface ocean, and temporal changes at selected locations. *Marine Chemistry*, *164*, 95–125. https://doi.org/10.1016/j.marchem.2014.06.004

Wahl, M., Saderne, V., & Sawall, Y. (2015). How good are we at assessing the impact of ocean acidification in coastal systems? Limitations, omissions. *Marine and Freshwater Research*, *67*, 25–36. https://doi.org/10.1071/MF14154

Yates, K. K., Dufore, C., Smiley, N., Jackson, C., & Halley, R. B. (2007). Diurnal variation of oxygen and carbonate system parameters in Tampa Bay and Florida Bay. *Marine Chemistry*, *104*(1–2), 110–124. https://doi.org/10.1016/j.marchem.2006.12.008

Yates, K. K., Rogers, C. S., Herlan, J. J., Brooks, G. R., Smiley, N. A., & Larson, R. A. (2014). Diverse coral communities in mangrove habitats suggest a novel refuge from climate change. *Biogeosciences*, *11*(16), 4321–4337. https://doi.org/10.5194/bg-11-4321-2014

Yeakel, K. L., Andersson, A. J., Bates, N. R., Noyes, T. J., Collins, A., & Garley, R. (2015). Shifts in coral reef biogeochemistry and resulting acidification linked to offshore productivity. *Proceedings of the National Academy of Sciences*, *112*(47), 14512–14517. https://doi.org/10.1073/pnas.1507021112